Advances in Colloid and Interface Science
94 (2001) 135–150

ADVANCES IN COLLOID AND INTERFACE SCIENCE

www.elsevier.com/locate/cis

Chains end-grafted in a theta-solvent and polymer melts: comparison of force–distance profiles

Lenore Lijun Cai[1], Steve Granick*

Department of Materials Science and Engineering, University of Illinois at Urbana, 105 South Goodwin Ave., Urbana, IL 61801, USA

Abstract

We find an unexpected analogy between polymer melts compressed between strongly-attractive solid surfaces, and end-attached polymers in near-theta-solvent. End-grafted polystyrene (PS) chains with various graft density were produced by immersing mica, coated with adsorbed diblock copolymers of PS/PVP, PS/polyvinylpyiridine, into *trans*-decalin at 24°C (this solvent is a near-theta-solvent for PS but a non-solvent for PVP), and the force–distance relations were measured using a surface forces apparatus. The end-grafted PS chains repelled one another in spite of the theta-solvent situation. Repulsive forces began at a thickness, per adsorbed layer, equivalent to 4–5 times the unperturbed radius of gyration of the PS chain. These cases of symmetrically-opposed PS layers are compared to the asymmetric case (PS on one mica surface, the other mica surface bare) and to the case of adsorbed PS homopolymer. Force–distance profiles in the presence of unattached PS homopolymer in solution at concentration c^* (the overlap concentration) displayed repulsion beginning at considerably larger separation than in the presence of pure solvent. Finally, we compare to confined melts of linear polydimethylsiloxane (PDMS), cyclic PDMS and a linear perfluoropolyether (Demnum). For these cases of polymer melts confined between adsorbing surfaces, force–distance relations could be described by the same functional relations as for end-attached chains in near-theta-solvent.

Keywords: Force–distance; Polystyrene (PS) chains; Theta-solvent; Surface; Polymer melt; Adsorption

* Corresponding author. Tel.: +1-217-333-1441; fax: +1-217-333-2736.
E-mail address: sgranick@uiuc.edu (S. Granick).
[1] Present address: PPG Industries, Inc., 4325 Rosanna Dr., Allison Park, PA 15101, USA.

0001-8686/01/$ - see front matter
PII: S0001-8686(01)00058-6

Contents

1. Introduction

Polymer chains that are end-attached to a surface at high density produce local segment concentrations so large that the tethered chains are obliged to stretch away from the surface to reduce their osmotic pressure. They present attractive model systems in which the chain configurations are nicely defined from several points of view: first, chains can be end-attached to have homogeneous conformations; secondly, the points of surface attachment are fixed; third, the graft density is controllable. All three points contrast with homopolymer adsorption. At the time this paper is written, more than two decades after the pioneering analysis of Alexander and de Gennes based on scaling ideas [1,2], study of the configurational structure of polymer brush systems is relatively mature and there exist definitive reviews [3–6]. Best understood of all are the static structure and surface forces of polymer brushes in good solvent conditions.

As concerns poor solvent conditions, Kent and co-workers reviewed literature in the context of neutron reflectivity and surface pressure measurements of brush thickness at variable temperature [7]. Perahia and co-workers studied wetting of a brush layer by polymer chains present in bulk solution [8]. Neutron scattering and reflectivity methods have been employed by Auroy and co-workers [9] and Karim and co-workers, [10] to study chain configurations. The resulting theoretical and computational situation was reviewed most recently by Grest [6]. But these experimental studies focused on the configurational statistics within single layers of polymer brushes.

Our problem here is different: forces of interaction between opposed brush layers in poor solvent conditions. Whereas in good solvent conditions force–distance relations have been studied thoroughly, concerning poor solvent conditions systematic studies do not appear yet to exist. This paper is devoted to doing so, and also to comparing to the case of polymer melts, which when deformed near an attractive surface over a time scale faster than required to equilibrate the chain

conformations, may be expected to form loops and tails with a distribution of end-attached lengths.

A parallel paper [11] concerns the response of end-attached chains in a near-theta-solvent to shear deformations.

2. Experimental

The surface forces apparatus was homebuilt after the design [12] of Israelachvili. To construct end-attached polymer chains, a convenient approach involves selective adsorption, in which one block of a diblock copolymer adsorbs strongly in a flattened conformation and the other block adsorbs negligibly. In this study, diblock copolymers of polystyrene and poly-2-vinylpyridine (PS-PVP) were studied while immersed in the near-theta-solvent, *trans*-decalin. Tirrell et al. [13] previously studied this same type of diblock copolymer in toluene, which is a non-solvent for PVP but a good solvent for PS. In the experiments described below, we found it convenient to allow the diblock copolymers to adsorb from toluene and then replace toluene by *trans*-decalin.

Characteristics of the PS-PVP diblock copolymers are listed in Table 1. We began with a polymer, Polymer A, generously donated by Professor Hiroshi Watanabe of Kyoto University. Later, to obtain higher grafting densities and longer brushes, we purchased Polymers B and C from Polymer Sources, Inc., Québec, Canada. All polymer samples were used as received. The *trans*-decalin (*trans*-decahydronaphthalene, purity 99%) was purchased from Fluka. The toluene (purity > 99.8%, HPLC grade) was purchased from Sigma–Aldrich. These solvents were stored before use over molecular sieves (5 Å, Aldrich) to remove trace moisture. In addition, to remove dust and other particulate matter, the solvents were filtered just before use through non-sterile 0.5-μm Millex-SR filters.

Muscovite mica has been used as the principal substrate in the surface forces apparatus since its introduction, owing to its atomic smoothness, optical translucency, and the ease by which clean surfaces may obtained for each new experiment simply by cleaving new samples. For adsorption onto mica, the PS/PVP solutions were prepared at concentrations 5–10 μg ml^{-1} in toluene — this was far below the critical micelle concentration in this solvent. It was known, from prior work, that the amount adsorbed is insensitive to concentration in this range of concentration [13]. The solutions were prepared at least 24 h before the adsorption process to ensure complete dissolution.

The bare mica sheets were first glued onto silica lenses using a 50:50 mix by weight of dextrose and galactose. The thickness of the bare mica sheets was calibrated in the surface forces apparatus, then the sheets were immersed in polymer solution for 2 h. (In experiments involving asymmetric brush layers, the mica thickness was calibrated after the experiment using different sheets of mica, cleaved at the same time and of identical thickness.) After adsorption, the surfaces were soaked in pure toluene for another 2 h. The preparations were performed within small glass vials outside the surface forces apparatus. For experiments where

Table 1
Characteristics of the PS/PVP diblock copolymers

Code	M_n, PS (g mol^{-1})	M_n, PVP (g mol^{-1})	M_w/M_n	R_G, PS[c] (Å)	σ_{dry} (chains per m^2)	Graft spacing[d] (Å)
Polymer A[a]	32 300	32 700	1.05	51	1.3×10^{16}	87
Polymer B[b]	52 500	28 100	1.07	65	1.1×10^{16}	95
Polymer C[b]	55 400	9200	1.03	67	3.4×10^{16}	54

[a] Donated by Professor Hiroshi Watanabe, Kyoto University, Japan.
[b] Purchased from Polymer Sources, Inc., Québec, Canada.
[c] Calculated from Brandup et al. [14].
[d] Calculated from dry thickness assuming same density as for bulk PS and PVP.

one mica surface contained end-attached polymer, and the other surface was bare, one sole surface was exposed to polymer solution during these ministrations.

After these adsorption and washing procedures, the coated surfaces were mounted within the surface forces apparatus. Toluene evaporated rapidly. Then a droplet of *trans*-decalin was introduced between the surfaces by pipette. The theta temperature of PS in bulk *trans*-decalin solution is 20°C [14], which is approximately 4°C below our experimental temperature of 24°C. The inside environment of the apparatus was kept dry by the presence of a hygroscopic chemical, P_2O_5 powder, and was kept saturated with solvent vapor by introducing droplets of *trans*-decalin to the bottom of the sample chamber. To prepare glassware for use, it was first soaked in concentrated nitric acid for at least 2 h and then rinsed with distilled water from a Barnstead Nanopure II filtering system. Manipulations were carried out under a laminar flow hood.

One tricky point was the need to control the water content of the solvent. Unless the solvent was dried over molecular sieves as described, it seemed that moisture competed with PVP for adsorption. The surfaces would begin to repel one another starting at a separation of several micrometers and visible black spots were observed under an optical microscope.

The graft density was inferred from the dry thickness. The polymer-laden surfaces were removed from the apparatus after finishing an experiment, rinsed with pure toluene to wash away *trans*-decalin, then dried under flowing argon gas for at least 3 h. The thickness of the dry layer was measured by multiple beam interferometry after remounting the surfaces into the surface forces apparatus. Assuming the same densities of PVP and PS as in the bulk, the grafting density was calculated from the thickness. In the experiments presented below, the quoted surface separation (D) refers to the separation of two polystyrene layers with the thickness of dry PVP (< 1 nm) subtracted.

3. Results and discussion

Force–distance profile in theta-solvent conditions. Fig. 1 shows a typical force–distance profile (Polymer C). The static force F that resists compression, normalized by the mean radius of curvature, R, of the crossed cylindrical surfaces, is plotted against surface separation, D. Initial experiments showed that 1–2 min was long enough to reach steady-state for each datum, so this was chosen as the equilibration time at each surface separation. The forces are evidently purely repulsive and the onset of repulsion was approximately 560 Å, which is eight to nine times the unperturbed radius of gyration ($R_G = 67$ Å) of PS with this molecular weight, in other words four to five times R_G per layer. Repulsion was observed starting at large separation in spite of the fact that the environment was a near-theta-solvent.

The thickness at the onset of repulsion is an important parameter in analyzing the structure of polymer brushes. Dividing the measured thickness by two gave the

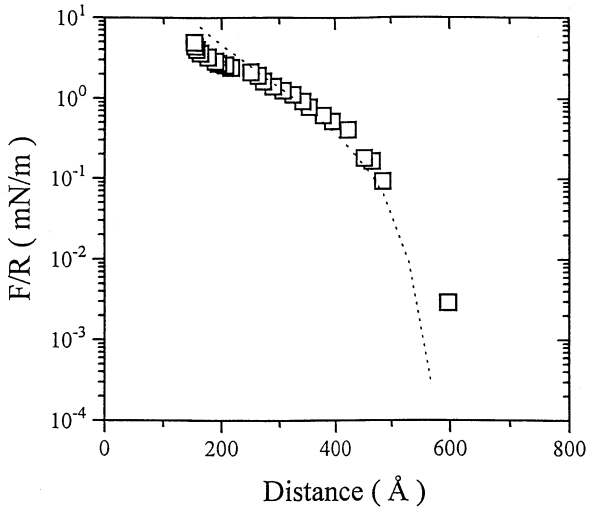

Fig. 1. The zero-frequency force that resists compression, F/R (force F normalized by the mean radius of curvature R of the opposed surfaces) is plotted logarithmically against surface separation for Polymer C. Squares show experiments. The dotted line shows the mean-field calculation based on the third virial coefficient estimated using Eq. (5) and Eq. (6).

unperturbed height of equilibrium polystyrene brushes of this molecular weight in this condition of solvent quality, $L_o = 280$ Å.

As a first attempt to describe the force–distance profile, we considered the seminal Alexander–de Gennes scaling theory [1,2], which established the main configurational features of polymer brushes, especially strong stretching normal to the surface. The extended length of an end-attached polymer, L_o, is predicted to follow the relation

$$L_o \sim Na\rho^{\nu} \tag{1}$$

where N is the number of repeat units of the chain, a is the statistical segment dimension of the repeat unit, and σ is the grafting density. The power-law component, ν, depends on the solvent quality; $\nu = 1/3$ under good solvent condition. If we follow Eq. (1) and assume the ideal theta condition ($\nu = 1/2$), it is straightforward to calculate the grafting density σ. The inferred result, using $L_o = 280$ Å and $a = 1.86$ Å, gives 2×10^{18} chains per m^2. This implies 7 Å between adjacent grafting points, which is unrealistic since it would imply more than unity values of volume concentration upon compressing together two opposed layers of end-attached chains. This is why we determined the graft density more directly from the thickness of the dried layers (see Section 2).

The local concentrations implied by the graft density were too small for the Flory–Huggins theory to hold except at the largest degrees of compression. Alternatively, the virial coefficients were considered. The free energy of compres-

sion was written as the sum of osmotic energy, f_{osmotic}, and elastic energy, f_{elastic}, where:

$$F_{\text{osmotic}}/k_{\text{B}}T \sim vN\varphi + wN\varphi^2 \tag{2}$$

$$F_{\text{elastic}}/k_{B}T \sim \tfrac{1}{2}L^2/R^2 \tag{3}$$

Here k_{B} is the Boltzmann constant, T is the absolute temperature, v is the second virial coefficient ($v = 0$ in theta conditions) and w is the third virial coefficient.

In the crossed-cylinder geometry of these experiments, the Derjaguin approximation [12] shows that the force $F(D)/R$ is 2π times the equivalent interaction energy between a unit area of parallel surfaces held at the surface separation of closest approach. Combining with Eq. (1), we write:

$$F(D)/R = 4\pi k_{\text{B}}T/a^2(w/2)^{1/2}N\sigma^2(D/2L_{\text{o}} - 2L_o/D) \tag{4}$$

The unknown parameter in Eq. (4) is the third virial coefficient — graft density (σ) and layer thickness (L_{o}) were measured. Conceptually, the third virial coefficient reflects the excess interaction of ternary clusters, but it is difficult to measure as it depends strongly on temperature, solvent quality and also molecular weight [15]. We sought to estimate, as follows, the third virial coefficient for polystyrene in *trans*-decalin at 24°C. Classically, the reduced third virial coefficient has been considered as:

$$g = w/v^2M \tag{5}$$

and it has been supposed that the value of g is constant. The value, $g = 0.25$–0.333, has been reported from various studies [16–18]. We took the value $g = 0.333$ according to polystyrene in cyclohexane solvent near the theta condition [18]. Unfortunately, we were unable to find studies of the molecular weight dependence of the third virial coefficient under theta-solvent conditions, but the molecular weight dependence of the third virial coefficient in good solvent has been reported [19] as:

$$w \sim M^{0.59} \tag{6}$$

The second virial coefficient has been measured to be $v = 9.53 \times 10^{-4}$ mol cm^3 g^2 for polystyrene of molecular weight 179 300 g mol^{-1} in *trans*-decalin at 30°C [14]. Combining Eq. (5) and Eq. (6), we estimate the third virial coefficient w for our system, $w \approx 2.6$. Uncertainties arise from the difference between our experimental temperature, which was slightly lower than the literature temperature as well as the use of molecular weight dependence for good solvent conditions. Fortunately, we expect the influence to be mitigated owing to the square root influence on w in Eq. (4).

We then calculated the expected $F(D)/R$ using Eq. (4). The dotted line in Fig. 1 compares the results of this calculation with the experiment. One sees that the

calculation fit the experimental data at low and moderate compression but deviated at high compression. A virial approach should be expected to fail when the local concentration becomes large, however.

It was assumed here that the theta temperature of PS in these confined spaces remained the same as for PS chain in the bulk. In a confined geometry, the influences of the surface-polymer and surface-solvent interactions may also contribute heavily, in addition to the conventional considerations of segment–segment interactions in solvent, which raises the possibility that the theta temperature in a confined space might change. Unfortunately, no reported work was been found that considers quantitatively the possibility of changes of the theta temperature of polymer solutions in confined spaces.

3.1. Comparison with a single layer squeezed against naked mica

Can one predict the structural forces owing to a single compressed layer simply by taking one-half of the interactions between two opposed layers? Is compression against an unyielding hard solid equivalent to compression against another polymer layer? To address this experimentally, the polymer was coated onto one sole mica substrate. The opposed surface was kept bare as described in the Section 2.

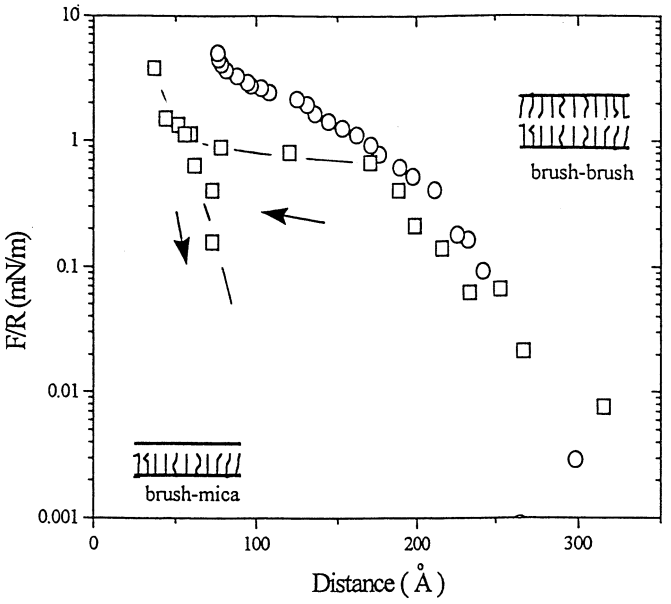

Fig. 2. Comparison of asymmetric (brush-against-mica) and symmetric (brush-against-brush) force–distance profiles for Polymer C. The equilibrated F/R is plotted logarithmically against surface separation. Circles denote brush-against-brush situation (same forces as Fig. 1 but the distance scale is divided by 2). Squares show the brush-against-mica situation upon compression (arrow pointing left) and upon separation (arrow pointing downward and to the right). The data deviate only when the force was large.

The force–distance profiles are compared in Fig. 2 (distances for the symmetric situation having been divided by two for the comparison). At low compression all of the data follow essentially the same curve. But it was easier to compress the single layer against bare mica and this was also associated with significant hysteresis. This may reflect some attraction of the dangling PS chains for the opposed surface. No quantitative description of the discrepancy is attempted at this time. The main point is agreement in the situation of mild overlap.

3.2. Dependence on graft density

Two additional samples of lower graft density were also studied (their characteristics are given in Table 1). The graft density was calculated from the dry layer thickness.

First we consider the force–distance profiles normalized by the unperturbed radius of gyration (Fig. 3). Just as in Fig. 1 we measured monotonic repulsion starting at large separations, but its onset at 3–5 R_G was at smaller relative separation than in Fig. 1. The scaling of these curves using Eq. (1) with the parameters appropriate to the theta-solvent condition is shown in Fig. 3. Here surface separation (D) has been normalized as suggested by Eq. (1) with exponents appropriate to the theta-solvent situation.

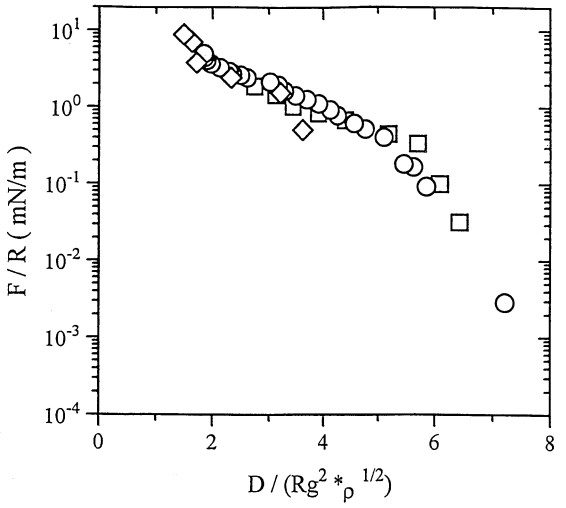

Fig. 3. Comparison of all three samples: Polymer A (circles); Polymer B (diamonds); and Polymer C (squares), using the scaling suggested by Eq. (1) with powers appropriate for theta-solvent conditions. The logarithmic force, F/R is plotted against surface separation normalized by the squared unperturbed radius of gyration of the PS chain multiplied by the square root of grafting density.

3.3. Confined melts (pseudo-brushes)

Owing to adsorption, both structural forces and shear rheology change significantly from the bulk behavior when unfunctionalized melt chains are confined to near-molecular spacings [20–22]. Here we revisit some previously unpublished data from this laboratory concerning strongly adsorbed polymers, and analyze it using Guiselin's 'pseudo-brush' model [23]. Under the assumption of irreversible adsorption, Guiselin predicted that loops within the adsorbed chains can be viewed as 'stretched' away from the surface, much as for a system of polydisperse polymer brushes. The Alexander–de Gennes 'blob' model was elaborated by considering the non-uniform size of 'blobs' with the result that static forces resisting compression were written as:

$$F(D)/R \sim k(2L_o/D - D/2L_o)^2 \tag{7}$$

where k is a constant, D is the surface separation and L_o is the onset of repulsion per layer.

To compare with experiments, Fig. 4 shows $F(D)/R$ plotted against surface separation for three systems of polymer melts confined between mica (all adsorb strongly to mica): linear polydimethylsiloxane (PDMS); cyclic PDMS; and a perfluorinated polyether. Molecular characteristics of these samples are given in Table 2. The similar shapes on semilogarithmic scales are suggestive. Upon replotting these data following the Guiselin prediction, Eq. (7), all show a linear relationship between $F(D)/R$ and $(2L_o/D - D/2L_o)^2$, which is consistent with the prediction. Here $2L_o$ is identified as the distance at onset of repulsion in the force–distance profile.

Fig. 5 shows this replotted data. Although the Guiselin theory was developed for linear polymers, interestingly the adsorbed cyclic polymer melts seem to follow this same functional relation.

Most of these polymers were not long enough to be strictly Gaussian chains (which was another assumption in the prediction). Also, the compression range of these polymer melts was small relative to that for the diblock copolymer systems. Still, this favorable comparison between data on polymer melts and the Eq. (7)

Table 2
Characteristics of the polymer melts

Sample	M_n (g mol^{-1})	M_w/M_n
Linear PDMS[a]	10 060	1.15
Linear PDMS[a]	14 760	1.11
Cyclic PDMS[a]	14 540	1.05
Demnum[b]	8000	1.09

[a] Polydimethylsiloxane, PDMS; values taken from Peanasky, S., PhD thesis, University of Illinois at Urbana-Champaign, 1995.

[b] Demnum, $(CF_2)_n$; values reported (private communication) by Dr Do Yoon, IBM.

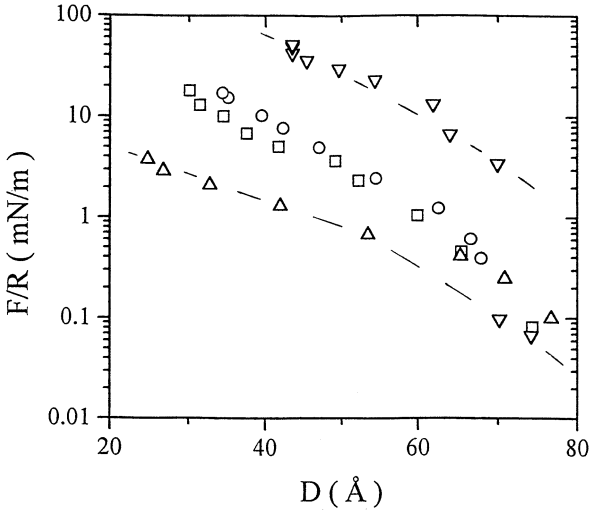

Fig. 4. Comparison with four polymer melts whose molecular characteristics are given in Table 2. The normalized steady-state force, F/R, evaluated after equilibration for 10–20 min per datum, is plotted logarithmically against surface separation for: linear PDMS with M_n = 10 060 (triangles up); linear PDMS with M_n = 14 760 (squares); cyclic PDMS with M_n = 14 540 (circles); and a perfluorinated polyether, Demnum with M_n = 8000 (triangles down). Dotted lines are guides for the eye.

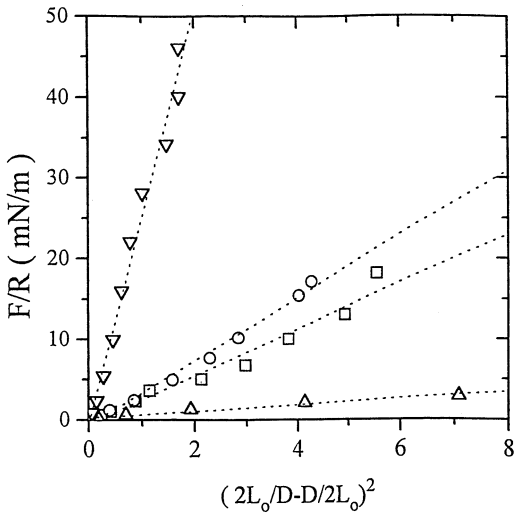

Fig. 5. Data replotted from Fig. 4 according to the relation suggested by Eq. (7). The ordinate is unchanged, but plotted on a linear scale. The horizontal axis was normalized using the Guiselin 'pseudo-brush' model with $2L_o$ identified as the distance at onset of repulsion in the force–distance profile. Symbols are the same as in Fig. 4.

based on the pseudo-brush model points the way to intriguing possibilities to use this scaling to describe end-attached of variable graft density and variable molecular weight.

As noted by a referee, the much stronger forces measured for the perfluorinated polyether, despite its low molecular weight, demonstrate the non-equilibrium nature of these forces. Qualitatively, the strong physisorption of polyether segments leads to a tighter non-equilibrium — a freezing-in of a broader distribution of macrostates than for PDMS.

3.4. Comparison to homopolymer of similar chain length adsorbed from solution

It becomes appropriate to compare to the case of adsorbed homopolymer: to the case of no point of preferential surface attachment. The adsorption of homopolystyrene onto mica in the vicinity of the theta temperature was studied previously by this laboratory under conditions of near-theta-solvent quality [24]. Seeking a realistic comparison with that situation, we chose a polystyrene homopolymer with $M_n = 37\,900$ g mol^{-1} ($M_w/M_n = 1.03$, obtained from Toyo–Soda). This molecular weight was close to the molecular weight of the polystyrene block in the sample PS/PVP-32–33. Adsorption was performed just as for the block copolymer, except from a toluene solution at the larger concentration of 1 mg ml^{-1}. After adsorption, the mica surfaces, coated with adsorbed polymer, were dried, mounted into the surface forces apparatus, and *trans*-decalin was added. The dry thickness at the end of measurements was 34 Å. Fig. 6 compares the force–distance profiles (for more direct comparison, the horizontal axis is plotted in mean concentration, ϕ_{PS} ($\phi \equiv D_{dry}/D$), rather than surface separation). Though the onset of repulsion was approximately the same in both systems, one notices that much less force was required to compress the adsorbed homopolymer. One might suspect that adsorbed homopolymer chains were squeezed out of the gap by compression, but this seems unlikely since no significant hysteresis or history dependence was observed.

3.5. Polymer solution exposed to the end-attached chains

End-attached chains were allowed to adsorb as described. Droplets of homopolymer solution were added. These consisted of 10% solutions by weight in *trans*-decalin of polystyrene ($M_n = 51\,000$ g mol^{-1}, $M_w/M_n = 1.02$, Toyo–Soda). The solutions were prepared at least 24 h before use to ensure complete dissolution. By the typical definition, $c/c^* \approx 1.4$.

The range of repulsion increased by a large amount, in spite of equilibrating the measurements for up to 10 times longer than in the earlier measurements (10–20 min at each datum). Fig. 7, Panel (a), shows $F(D)/R$ plotted against surface separation, D. If one follows the compression curve, one notices that the onset of repulsion appeared at D twice as large as for the brush in pure solvent. Also the magnitude of repulsion was approximately 10 times as large as for the brushes.

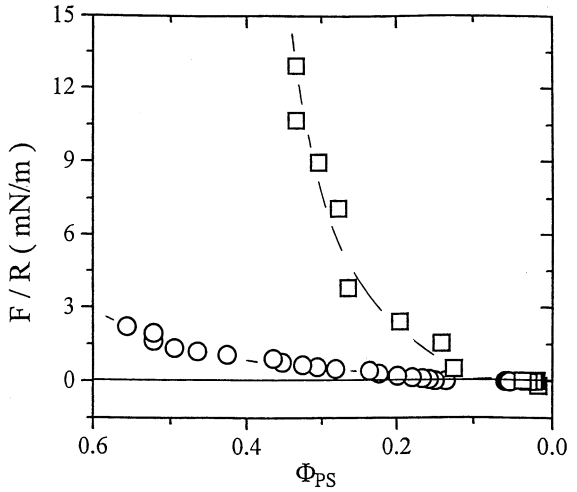

Fig. 6. Forces that resist compression, F/R, plotted against the estimated mean interfacial polymer concentration of polystyrene, ϕ_{PS}, ($\phi_{PS} \equiv D_{dry}/D$) calculated from the measured thickness of the dried layers. The data concern unfunctionalized polystyrene homopolymer (circles), M_n = 37 900 g mol^{-1}, measured in *trans*-decalin after adsorption from toluene solution at concentration 1 mg ml^{-1} as described in text, and Polymer A (squares).

This may reflect homopolymer chains that dangled out of the brush structure into the solution, but were partially intertwined with it.

If one now follows the curve for decompression, it is interesting to notice substantial hysteresis — the data were the same as for compression only to $D \approx 600$ Å. This is suggestively close to the thickness of two brush layers measured in pure solvent.

If we suppose that at the larger thickness, the enhanced repulsion reflected the presence of homopolymer chains, one way to seek to quantify this effect was to subtract the measured forces by the forces measured at $D \approx 600$ Å, then to compare the remainder to forces measured for brushes in pure solvent. The comparison, shown in Fig. 7, Panel (b), demonstrates that compression of polymer brushes in the homopolymer environment was decidedly harder than the compression of these same brushes in pure solvent.

Comparable studies do not appear to have been performed previously in a theta-solvent environment. In good solvent, recent work by Auroy and Auvray [25] using small-angle neutron scattering (SANS), studied the influence of polymer solutions on the thickness of a single brush substrate. They observed shrinkage of the brushes, an effect attributed to enhanced osmotic pressure in the solution, but at higher solution concentrations than in our present experiments. Our data show no evident change, in the presence of polymer solution, of the thickness; the discrepancy between compression and decompression curves occurred at the same thickness as in pure solvent. Additional experiments using higher polymer concen-

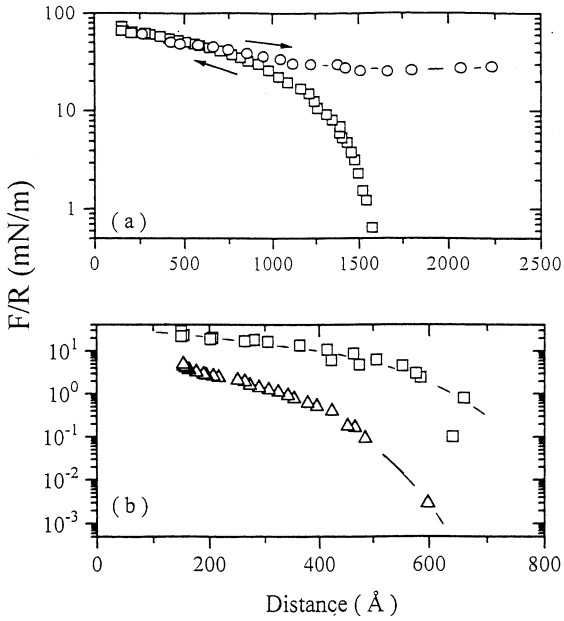

Fig. 7. Force–distance profiles for Polymer A immersed in a solution of PS homopolymer at 10% concentration in *trans*-decalin (same homopolymer as in Fig. 6). Squares show data during compression; circles show data upon separating the surfaces. Points were equilibrated for 10–20 min per datum. In Panel (b), these data are compared with the force–distance profile for Polymer A in polymer-free solution. The triangles repeat the data as in Fig. 1. The squares are obtained by subtracting, from the data shown in Panel (a), the forces measured at $D = 600$ Å.

tration will be desirable, though difficult technically in view of the higher viscosity of those solutions.

The system of polymer brushes immersed in a solution of mobile homopolymers has also been studied by Zhulina et al., using self-consistent field theory [26]. As the main purpose, in this experiment, was to test for the presence or absence of a strong effect, the data presented here demonstrates the existence of a strong effect. Though the experiments are difficult (equilibration times are so long that exceptional apparatus stability was needed to perform these measurements), the effect deserves further, more systematic, experimental as well as theoretical analysis. The possibility of hydrodynamic influences on the measured forces cannot be entirely discounted in spite of the fact that the fact that the forces had equilibrated on the experimental time scale of 10 min.

4. Outlook

This study has compared the force–distance relations of end-attached polymer

chains in good solvent [1–6] to several less-studied cases, especially to end-attached polymers in near-theta-solvent. In comparing the three systems of end-attached diblock copolymers of different block lengths, Polymers A, B and C, the semantic question was intentionally avoided of what constitutes a 'brush' and what constitutes a 'mushroom' conformation. A careful analysis of the border between these regimes was presented recently [27].

We find an unexpected analogy to polymer melts compressed between strongly-attractive solid surfaces.

Looking to the future, and to a phenomenon that seems not yet to have been considered by careful theory, we find that the situation of end-attached chains, in the presence of unattached chains at $c \approx c^*$, presented repulsion at considerably larger separations than in the presence of pure solvent.

Acknowledgements

We are indebted to Professor Hiroshi Watanabe (Kyoto University) for the gift of a polymer sample. This work was supported by the National Science Foundation (Tribology Program).

References

[1] S. Alexander, J. Phys. (Paris) 38 (1977) 983.
[2] P.-G. de Gennes, C. R. Hebd. Seances Sci. 300 (1985) 839.
[3] S.T. Milner, Science 251 (1991) 905.
[4] A. Halperin, M. Tirrell, T.P. Lodge, Adv. Polym. Sci. 100 (1992) 31.
[5] I. Szleifer, M.A. Carignano, Adv. Chem. Phys. 94 (1996) 165.
[6] G.S. Grest, Adv. Polym. Sci. 138 (1999) 149.
[7] M.S. Kent, J. Majewski, G.S. Smith, L.T. Lee, S.K. Satija, J. Chem. Phys. 110 (1999) 3553.
[8] D. Perahia, D.G. Wiesler, S.K. Satija, L.J. Fetters, S.K. Sinha, S.T. Milner, Phys. Rev. Lett. 72 (1994) 100.
[9] P. Auroy, L. Auvray, L. Léger, Macromolecules 24 (1992) 2523.
[10] A. Karim, V.V. Tsukruk, J.F. Douglas et al., J. Phys. II Fr. 5 (1995) 1441.
[11] L.L. Cai, S. Granick, to be submitted.
[12] J.N. Israelachvili, Intermolecular and Surface Forces, 2nd, Wiley, New York, 1992.
[13] M. Tirrell, E. Parsonage, H. Watanabe, S. Dhoot, Polym. J. 5 (1991) 641.
[14] J. Brandup, E.H. Immergut, E. Grulke, A. Abe, D. Bloch (Eds.), Polymer Handbook, Wiley, New York, 1999.
[15] H. Fujita, Polymer Solutions, Elsevier Science Publishers, New York, 1990.
[16] P.J. Flory, Principles of Polymer Chemistry, Cornell Univ. Press, Ithaca, NY, 1953.
[17] G.C. Berry, J. Chem. Phys. 48 (1968) 2103.
[18] H. Vink, Eur. Polym. J. 10 (1974) 149.
[19] K.R. Kniewske, W.H. Kulicke, Makromol. Chem. 184 (1983) 2173.
[20] S. Granick, H.-W. Hu, Langmuir 10 (1994) 3857.
[21] S. Granick, A.L. Demirel, L. Cai, J. Peanasky, Isr. J. Chem. 35 (1995) 75.
[22] S. Granick, Phys. Today 52 (1999) 26.

[23] O. Guiselin, Europhys. Lett. 17 (1992) 225.
[24] H.-W. Hu, S. Granick, Macromolecules 23 (1990) 613.
[25] P. Auroy, L. Auvray, Macromolecules 29 (1996) 337.
[26] E.B. Zhulina, O.V. Borisov, L. Brombacher, Macromolecules 24 (1991) 4679.
[27] K. Kunz, S.H. Anastasiadis, M. Stamm, T. Schurrat, F. Rauch, Eur. Phys. J. B7 (1999) 411.